Pergamon

*Applied Geochemistry*, Vol. 9, pp. 583–595, 1994
Copyright © 1994 Elsevier Science Ltd
Printed in Great Britain. All rights reserved
0883–2927/94 $07.00 + 0.00

0883–2927(94)E0016–X

# Kinetic modelling of geochemical processes at the Aitik mining waste rock site in northern Sweden

BO STRÖMBERG

Department of Chemical Engineering, The Royal Institute of Technology, S-100 44 Stockholm, Sweden

and

STEVEN BANWART

Department of Inorganic Chemistry, The Royal Institute of Technology, S-100 44 Stockholm, Sweden

(*Received* 19 *September* 1993; *accepted in revised form* 25 *March* 1994)

**Abstract**—A steady-state geochemical model has been developed to study water–rock interactions controlling metal release from waste rock heaps at the Aitik Cu mine in northern Sweden. The Cu release in drainage waters from the site is of environmental concern. The waste rock heaps are treated as single completely mixed flow-through reactors. The geochemical model includes kinetices of sulphide and primary silicate mineral weathering, heterogeneous equilibrium with secondary mineral phases and speciation equilibrium. Field monitoring of drainage water composition provides a basis for evaluation of model performance.

The relative rate of oxidative weathering of sulphides and dissolution of primary silicate minerals, using published kinetic data, are consistent with net proton and base cation fluxes at the site. The overall rate of $Fe^{2+}$ oxidation within the heap is three orders of magnitude faster than that which could be explained by surface-catalysed reaction kinetics. This suggests significant activity of iron-oxidizing bacteria. The absolute weathering rates of sulphides and silicate minerals, normalized to a measured BET surface area, are approximately two orders of magnitude lower at field scale than published rates from laboratory experiments. Because of the relative absence of carbonate minerals, the weathering of biotite and plagioclase feldspar are important sources of alkalinity.

## INTRODUCTION

THE mobility, reactivity and bioavailability of trace elements within the hydrologic cycle is critically dependent on the aqueous speciation controlling their solubility and sorption behaviour. Because speciation is a function of the master variables pH and Eh it is necessary to understand the coupled biological and geochemical reactions controlling the pH buffer system and redox conditions in natural waters.

The global electron balance represented by the present-day reservoir of molecular oxygen, is maintained at an average steady state by the relative rates of photosynthesis, respiration, oxidative weathering of crustal minerals (sulphides, elemental carbon) and volcanic input of volatile reductants ($H_2S$ and $SO_2$; HOLLAND *et al.*, 1986). Because proton transfers accompany electron transfers in order to maintain charge balance, electron cycling results in an associated modification of the proton balance (STUMM *et al.*, 1983). The atmosphere is thus characterized as an oxidizing, acidic environment relative to the geosphere and its enormous reservoir of mineral bases and reductants.

Local perturbations of these global chemical cycles can result in significant, but spatially limited, environmental degradation. A well-known example is the mobilization of heavy metals from waste sulphide ores at open mine sites. In the process of ore extraction, large amounts of crushed waste rock are left exposed to the atmosphere. Accelerated weathering of sulphide minerals by $O_2$ under surface hydrologic conditions can result in critical loading of soluble toxic metals on local and regional scales.

Sweden has a history of extensive mining of copper sulphide ore, dating back to the 13th century. Mining waste deposits from early ore extraction (e.g. Bersbo site; KARLSSON *et al.*, 1988) as well as those at currently operating mines must be evaluated in terms of contamination potential and possible remediation strategies. Here we present results from initial site investigations and geochemical modeling of processes in waste rock heaps at the Aitik site in northern Sweden.

Important chemical processes within the waste rock heaps include generation of free acidity and soluble metal species through oxidative weathering of sulphide minerals. At the Aitik site, pyrite ($FeS_2$) and chalcopyrite ($CuFeS_2$) are dominant reservoirs of reduced sulphur and Cu, respectively. The proton balance is controlled by the relative rates of acidity generation and alkalinity production by weathering

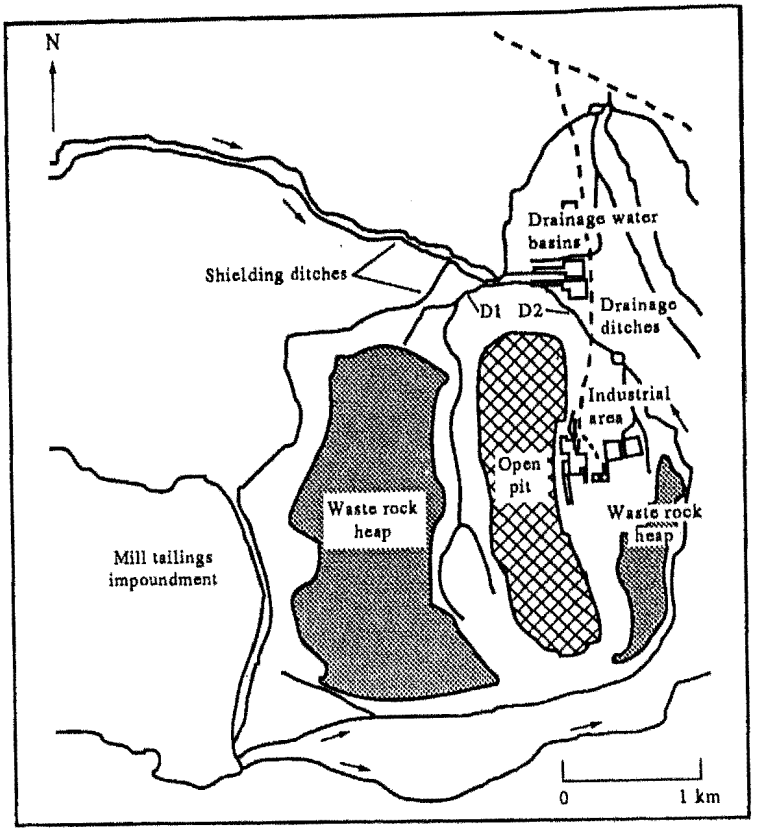


FIG. 1. Map of the Aitik open pit mine with surroundings. Samples of drainage water from the waste rock heaps were collected in the ditches marked D1 and D2. The open pit is represented by the hatched area in between the waste rock heaps.

of primary silicate minerals. Although calcite dissolution can provide a rapidly accessible reservoir of alkalinity, we have demonstrated with large-scale laboratory column experiments (0.8 m diameter × 2 m) that the trace amounts present in fresh waste rock from this site should be depleted within the waste rock heaps on a time scale of not more than a few years (STRÖMBERG *et al.*, 1994).

Previous approaches for predicting release of metals have focused on rate-limiting $O_2$ diffusion through a sulphide depleted mineral surface layer ("shrinking core model"; LEVENSPIEL, 1972) coupled with surface chemical reaction kinetics (BARTLETT, 1992; DIXON and HENDRIX, 1993), microbially catalysed kinetics (HERRERA *et al.*, 1989), diffusion through pore space between particles (DAVIS and RITCHIE, 1986) or air convection between particles (CATHLES and APPS, 1975; PANTELIS and RITCHIE, 1991). The relative importance of these processes is expected to be affected by the particle size distribution, mineralogy, temperature and hydrologic conditions. These are related to the nature of the mining waste, the site characteristics, and the time scale of interest; months, decades, lifetime of the waste deposit.

This study provides a steady-state model for the prevailing geochemical conditions at the Aitik waste rock deposit. The model includes weathering of sulphides and primary silicate minerals, aqueous speciation equilibrium, formation of secondary mineral phases and advective transport. Mineral weathering is treated as surface chemical controlled kinetics. This assumption is expected to be valid as long as exposed mineral surfaces have not been significantly altered. The objectives of this study are:

(1) to present site description and literature data relevant to geochemical modeling of the Aitik waste rock deposit;

(2) to develop a geochemical model for leachate genesis and element cycling at the site;

(3) to compare model results with drainage water composition as a critical evaluation of model performance and knowledge of ongoing geochemical processes.

## SITE DESCRIPTION

The Aitik site located near Gällivare in the north of Sweden, operated by Boliden Mineral AB, is currently Europe's largest copper mine (Fig. 1). The waste rock is disposed close to the open pit on an area extending 400 ha, whereas the mill tailings are pumped to an impoundment in a nearby valley. The waste rock is removed from the open pit in order to reach ores enriched in metals above the

economic cutoff. Waste materials generated from the ore extraction are 14 million metric tonnes of waste rock each year and approximately the same quantity of mill tailings, i.e. the ratio of waste rock removed compared to ore processed is approximately 1:1.

No vascular plants exist on the Aitik waste rock heaps. A fraction of the east waste rock heap is covered with moraine. For the rest of the waste rock deposits no cover layers have been installed at present. A programme for assessing protective measures after mining activities cease is being carried out (Boliden Mineral AB, ANSTO, Golder Geosystem).

The waste rock heaps are unsaturated with moisture and have remained predominantly oxic according to measured oxygen levels in the poregas (Bennett *et al.*, 1992). The rate of sulphide oxidation is low in comparison with rate of oxygen transport in heap poregas and is such that the 15 m high dumps remain aerated over their full height. After the first 10 months of field measurements, a majority of monitoring holes had oxygen levels of 10–20 vol. %. The lowest level which was detected is 3 vol. %. An estimated average oxygen level of 10 vol. % is used in the model calculations. Similar measurements at other waste rock deposits have shown that oxygen levels are often lower (Harries and Ritchie, 1985; Bennett and Ritchie, 1991; Gélinas *et al.*, 1992). For mill tailings impoundments with smaller particle sizes, and often higher abundance of sulphide minerals, anoxic conditions may dominate (Blowes *et al.*, 1991).

The average precipitation in the area is 0.68 m $a^{-1}$. As the surface of the waste rock deposits is primarily composed of large pieces of rock (diameter >0.1 m), rapid infiltration and a low average temperature results in low evaporation. A net infiltration rate of 0.5 m $a^{-1}$ has been estimated (Axelsson *et al.*, 1992). The annual average temperature in the area is 0°C, with average summer temperatures at 15°C and average winter temperatures at −15°C. The temperature within a waste rock deposit may be affected by the exothermic sulphide oxidation as shown by Harries and Ritchie (1981). Measurements at the Aitik site show a temperature variation between −5 and 12°C near the surface of the rock waste heaps and an almost constant temperature of 0–3°C at the base (Bennett *et al.*, 1992). Outflowing steam from restricted areas of the heap surface indicate that local spots have higher temperatures, which may reflect internal heat sources from sulphide oxidation. An average temperature of 5°C was estimated and used in the model calculations presented below.

The drainage water from the waste rock deposits is collected in ditches and then used as process water in the enrichment plant. Hydrologic investigations and groundwater monitoring in the area indicate that only a small fraction of drainage water from the waste rock heaps infiltrates the subsurface (Axelsson *et al.*, 1992). The drainage water in the two main ditches D1 and D2 (Fig. 1) is regularly analysed for major components. Average flowrate and chemical composition after 2 a of field measurements are given in Table 1. Samples were collected from the ditches in polyethylene bottles (0.5 l), autoclaved (200 kPa, 30 min) and analysed within 1 week. Soon after autoclaving, a portion of each sample was acidified (10 ml conc. $HNO_3$ to 40 ml sample) for subsequent analysis. Duplicate analysis on samples filtered (0.2 $\mu$m pore-diameter cellulose acetate membrane filters) prior to acidification, and unfiltered acidified samples showed no difference in dissolved metal concentration. Total concentrations of dissolved metals Cu, Zn, Mg, Fe, Al, Mn and Ca were measured using inductively coupled plasma–atomic emission spectroscopy (ICP–AES, ARL-3580). Flame atomic absorption spectroscopy (Perkin-Elmer 100B) was used to analyse K, Na and Sr, and graphite furnace atomic absorption spectroscopy (Perkin-Elmer 5000/Zeeman instrument) was used to analyse Pb, Cd and Ni. Silicon was determined spectrophotometrically using molybdenum blue as chromogen. Anions were analysed using a Tecator 6200 ion chromatograph. For some of the samples, ion chromatography was also used to analyse previously mentioned base cations and trace elements (Dionex DX-300 with variable wavelength detector-II and conductivity detector-3). Alkalinity was determined by volumetric titration of unacidified samples by strong acid to the $H_2O$–$CO_2$ endpoint, and is reported as bicarbonate ion concentration. Proton activity was measured using a combined glass electrode–Ag/AgCl(s) reference electrode system (Metroohm 691) calibrated with standard buffer solutions at pH 4 and 7.

Table 1. Characterization of drainage water composition and flowrates in the two main drainage ditches D1 (west ditch) and D2 (east ditch). Mean concentrations ±1 S.D. (mg/l)*

| | D1 | D2 |
|---|---|---|
| pH | 3.8 ± 0.1 | 4.2 ± 0.4 |
| $SO_4$ | 1310 ± 250 | 220 ± 97 |
| Ca | 185 ± 46 | 47 ± 24 |
| Mg | 57 ± 13 | 11 ± 5.7 |
| Al | 75 ± 24 | 6.5 ± 4.4 |
| Cu | 19 ± 5.0 | 1.2 ± 0.8 |
| Fe | 2.0 ± 1.0 | 2.8 ± 1.9 |
| Zn | 5.8 ± 1.6 | 0.40 ± 0.3 |
| Na | 46 ± 9.0 | 14 ± 7.4 |
| K | 17 ± 4.5 | 4.2 ± 2.0 |
| Si | 19.1 ± 7.1 | 16.4 ± 8.6 |
| Cl | 27 ± 8 | 5.5 ± 3.5 |
| Mn | 12.1 ± 3.9 | 2.2 ± 1.6 |
| Ni | 1.3 ± 0.7 | 0.17 ± 0.20 |
| Co | 1.1 ± 0.2 | 0.16 ± 0.15 |
| $NO_3$-N | 8.2 ± 3.1 | 0.49 ± 0.26 |
| $HCO_3$ | <0.05 | <0.05 |
| Flowrate ($m^3$/min)† | 10 (2–50) | 2 (0.5–10) |

*Chemical analysis was carried out on 33 and 30 samples from ditch D1 and D2, respectively. Samples were taken between May 1991 and October 1993, where $SO_4$, Ca, Mg, Cu, Zn, Al, Fe and pH were analysed on each occasion. For other components in the table, between five and eight selected samples from each ditch were analysed. Trace concentrations of Pb (<0.30 mg/l), Cd (<0.02 mg/l) and Sr (<0.9 mg/l) were also detected.

†Mean value and upper and lower limits for 42 observations made between May 1991 and May 1993 using gauge heights.

Flowrates and concentrations of major components in the two drainage water ditches are nearly constant during the year except for a period in the spring when flowrates increase by up to an order of magnitude and concentrations drop by a factor of 2–10. In estimating mass fluxes of elements from the waste rock heaps, a time and space integrated composition is required. The water composition in the west ditch (D2), draining the largest waste rock heap (250 ha), represent 85% of drainage water flow from the site and will subsequently be used. In addition to waste rock drainage water, ditch D2 intercepts seepage water from the tailings impoundment and infiltration from the surrounding catchment area. This causes a dilution of drainage water from the waste rock heaps. Using the limited information available on composition of seepage water (Jönsson, pers. comm. 1993) and relative flowrates (Axelsson *et al.*, 1992) suggests that the differences between total concentrations in the ditches and corresponding concentrations in waste rock drainage water are not larger than a factor of 2.

We define acidity in this system as the base neutralizing capacity (BNC) with respect to the $CO_2$–$H_2O$ reference proton level [Eqn (1)]. Alkalinity is defined as the corresponding acid neutralizing capacity (ANC):

Table 2. Mineral composition of fresh waste rock in volume %

| Mineral | $v_i$ (mean ±1 S.D.) |
|---|---|
| Quartz | 24 ± 14 |
| K-feldspar | 24 ± 19 |
| Albite* | 13 ± 10 |
| Anorthite* | 6 ± 4 |
| Muscovite | 10 ± 16 |
| Biotite | 8 ± 7 |
| Skarn minerals† | 6 ± 18 |
| Accessory minerals† | 5 ± 7 |
| Calcite | 0.1 ± 0.5 |
| Pyrite‡ | 0.57 (0.08–1.7) |
| Chalcopyrite‡ | 0.09 (0.02–0.3) |

*Anorthite and albite form a plagioclase with composition close to oligoclase (Ab. 70%, An. 30%; BERGSTRÖM, 1981).

†Skarn minerals are amphibole, sphene and epidote. Accessory minerals are tourmaline, garnet, chlorite, apatite and scapolite. A minor fraction of pegmatite with low sulfur and copper content is excluded.

‡Abundance of pyrite and chalcopyrite is estimated from total sulfur and copper content of waste rock. The upper limits given correspond to the content of biotite gneiss and muscovite schist and the lower limits to skarnbanded gneiss. The uncertainty in the determination of copper and sulphur was estimated to be 10% (LARSSON, 1992).

$$BNC = [H^+] - [HCO_3^-] - 2[CO_3^{2-}] - [OH^-]. \quad (1)$$

The bedrock of the Aitik site is composed predominantly of gneisses of schists. The main rock type of the ore deposit is biotite gneiss whereas the waste rock also contains sericite to muscovite schist and skarn-banded gneiss, from the surrounding bedrock. Pyrite and chalcopyrite are the dominating sulphides with traces of pyrrhotite, sphalerite and bornite.

The abundance of rock-forming minerals has previously been determined from point counting using optical microscopy in transmitted and reflected light, on thin sections obtained from bore hole cores (BERGSTRÖM, 1981, 1982). Results from 70 thin sections corresponding to the part of the bedrock which is crushed as waste rock provide point estimates and variability in mineral composition (Table 2). Elemental analysis of individual minerals was carried out on 12 samples using electron microprobe analysis on representative samples prepared for examination by scanning electron microscopy. Total elemental composition of waste rock was analysed with powder XRF (Philips 1600). Total sulphur was also analysed with combustion in oxygen (Leco). Table 2 lists total volume % for the waste rock heaps as a weighted average using mineral composition and relative amounts of dominating rock types (LARSSON, 1992). The relatively large spatial variability in mineral composition is related to the banded structure of the formation.

Using the composition of drainage water (Table 1), speciation calculations were carried out using the geochemical code PHREEQE (PARKHURST *et al.*, 1980) with the original WATEQ database (TRUESDELL and JONES, 1974) and subsequent revisions summarized and critically reviewed by NORDSTROM *et al.* (1991). These calculations indicate the drainage water to be at or near saturation with respect to kaolinite [$Al_2Si_2O_5(OH)_4$(s)]. Iron speciation indicates either saturation or oversaturation with respect to Fe(III) oxyhydroxide (assuming equilibrium with the atmospheric $O_2$ reservoir in open ditches). In the following model development, $Fe^{3+}$ is maintained in equilibrium with Fe(III) oxyhydroxide and $Fe^{2+}$ concentration is controlled by the relative rates of Fe(II)-mineral dissolution and subsequent oxidation by $O_2$.

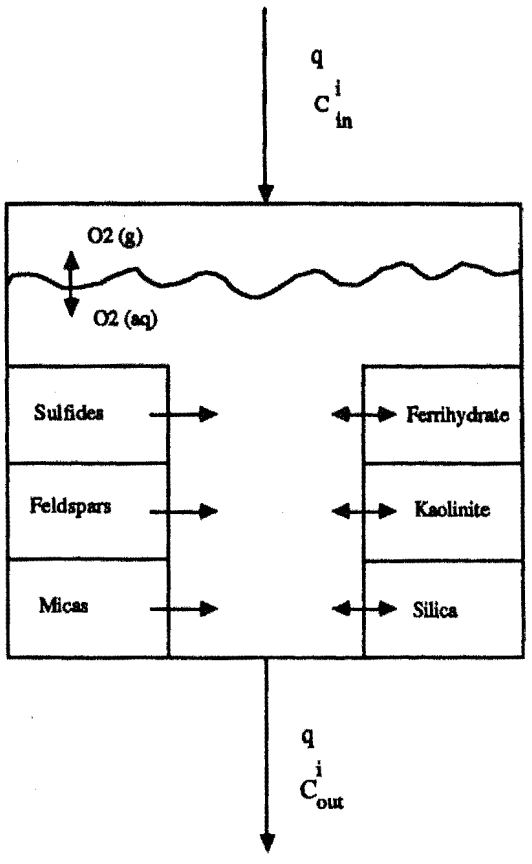


FIG. 2. The geochemical model is based on a completely-mixed flow-through reactor at steady state. Kinetically controlled weathering of primary and sulfide minerals is shown as one-sided arrows. Precipitation of secondary minerals and oxygen transfer from gas phase, controlled by equilibrium, is shown as two-sided arrows.

Drainage waters were also well above saturation with respect to alunite [$(KAl_3(SO_4)_2(OH)_6$(s)] and jarosite [$(K,Na,H_3O)Fe_3(SO_4)_2(OH)_6$(s)] (thermodynamic data from ALPERS *et al.*, 1989; VLEK *et al.*, 1974). Such mineral oversaturations in acid mine waters have been encountered elsewhere (NORDSTROM *et al.*, 1979) and may indicate a kinetic barrier to precipitation. Calculations using thermodynamic data for Cu-bearing secondary phases indicate oversaturation with respect to cupric ferrite [$CuFe_2O_4$(s); VIEILLARD, 1988]. As is commonly encountered for terrestrial waters, silica speciation indicates equilibrium with a solid phase exhibiting solubility between that of quartz and amorphous $SiO_2$(s). It is important to note that speciation calculations do not consider kinetics of heterogeneous reaction, co-precipitation equilibrium, non-idealities in solid phase behaviour or the actual presence of mineral phases.

## MODEL DEVELOPMENT

We have developed a model for leachate genesis using the geochemical code STEADYQL (FURRER *et al.*, 1989, 1990), which formulates slow reaction kinetics with empirical rate laws and rapid reactions as speciation equilibrium, for a single completely-mixed flow-through reactor at steady state (Fig. 2). This

reactor configuration neglects spatial and temporal variability in site geochemistry and hydrology. This modelling approach is justified because of the oxic conditions throughout the Aitik waste rock heaps, i.e. both acidity generating sulphide oxidation and pH buffering reactions occur throughout the whole height of the heaps. For water–rock interactions we have used the assumption of partial equilibrium (HELGESON, 1968, 1979; HELGESON *et al.*, 1969), when dissolution kinetics of primary and sulphide minerals are treated as irreversible processes far from equilibrium, and secondary phases are maintained in equilibrium with the aqueous phase. The program calculates steady-state concentrations of aqueous species and area specific fluxes for components.

*Mathematical description*

Speciation equilibrium is defined by the following general mass action equation where $C(i)$ is molar concentration of species $i$; $K(i)$ is the conditional stability constant; $X(j)$ is free concentration of component $j$ and $a(i,j)$ is the stoichiometric coefficient of component $j$ in species $i$:

$$C(i) = K(i) \prod_j X(j)^{a(i,j)}. \quad (2)$$

Free component concentrations are defined with a fixed activity (such as an activity of one for solid phases) or by the relative rates of chemical and transport processes at steady state. The general rate equation for a mobile component flux is as follows, where $J$ is the flux of component $j$ due to processes $l$, $s(l,j)$ is the stoichiometric coefficient of component $j$ in process $l$, $P(m)$ is the value of rate parameter $m$, and $n(l,i)$ is exponent of species $i$ in rate expression $l$:

$$J(l,j) = s(l,j) \prod_m P(m) \prod_i C(i)^{n(l,i)}. \quad (3)$$

Component fluxes due to outflow are distinguished from other processes and defined as follows, where $q$ is water flow rate through the cell:

$$J(\text{out},j) = -q \sum_i a(i,j)C(i). \quad (4)$$

The program iterates until convergence of difference functions $Y(j)$ is reached [$Y(j) \rightarrow 0$], or terminates after a specified number of interations. A more detailed mathematical description is given in FURRER *et al.* (1989, 1990):

$$Y(j) = q \sum_l J(l,j). \quad (5)$$

*Equilibrium speciation*

The equilibrium speciation model is given in Table 3. The choice of components reflects major element composition of leachate from the site (Table 1). Due to the limited literature data available on dissolution rates, we could not include Mn and Zn, which probably originate from weathering of the minor amounts of garnets and epidote, and sphalerite, respectively. Because sampled waters are greatly undersaturated with respect to secondary Zn-bearing phases, the geochemical behaviour of Zn should be conservative and analogous to that of Cu in the modeling study. Redox speciation of Fe is included by defining both $Fe^{2+}$ and $Fe^{3+}$ as components, with $Fe^{3+}$ concentration maintained in heterogeneous equilibrium with Fe(III) oxyhydroxide. The aqueous concentration of $H_4SiO_4$(aq) and $Al^{3+}$ are maintained simultaneously in heterogeneous equilibrium with $SiO_2$(s) and kaolinite. These assumptions are based on the speciation calculations of site drainage waters and mineralogical investigations. Concentration of $O_2$(aq) is assumed in equilibrium with an estimated average $pO_2$ in pore gas, based on site measurements (BENNETT *et al.*, 1992). All redox reactions are treated as slow kinetic processes.

*Kinetic processes*

The stoichiometry and rate laws for slow kinetic processes are given in Tables 4 and 5, respectively. Rate constants (Table 6) have been corrected with the Arrhenius expression to the estimated average heap temperature of 278 K. The utilized activation energies for sulphides [88–92 (kJ/mol); NICHOLSON *et al.*, 1988; WIERSMA and RIMSTIDT, 1984] are more than twice that reported for feldspars [35–38 (kJ/mol); WIELAND *et al.*, 1988]. For biotite and muscovite, we used an average activation energy for surface controlled dissolution of 60 (kJ/mol), suggested by LASAGA (1984).

The inflow (process 1) corresponds to the annual average precipitation at the site, and with an assumed corresponding acid deposition load. The rate law for oxidation of ferrous iron (process 2; WEHRLI, 1990) considers the abiotic reaction in solution and heterogeneous oxidation of Fe(II) adsorbed at mineral surfaces. Surface speciation for adsorbed Fe(II) was modelled using data from ZHANG *et al.* (1992) for surface complexation of Fe(II) on lepidocrocite. Total concentration of Fe(II) adsorption sites are calculated by using a site density of 3 $\mu$mol/m$^2$ (ZHANG *et al.*, 1992) and the total reactive surface area of the waste rock discussed below. Using the total reactive surface area provides an upper limit for adsorbed Fe(II) oxidation rate.

The rates of mineral dissolution were treated using empirical rate laws based on published laboratory weathering experiments. The rate laws for weather-

Table 3. Equilibrium speciation*

| Phase | log $K$† |
|---|---|
| **Aqueous phase** | |
| $H_2O - H^+ = OH^-$ | −14.5 |
| $H^+ + SO_4^{2-} = HSO_4^-$ | 1.43 |
| $Na^+ + SO_4^{2-} = NaSO_4^-$ | 0.22 |
| $K^+ + SO_4^{2-} = KSO_4^-$ | 0.31 |
| $Mg^{2+} + H_2O - H^+ = MgOH^+$ | −12.4 |
| $Mg^{2+} + SO_4^{2-} = MgSO_4^0$ | 1.47 |
| $Ca^{2+} + H_2O - H^+ = CaOH^+$ | −13.7 |
| $Ca^{2+} + SO_4^{2-} = CaSO_4^0$ | 1.56 |
| $Ca^{2+} + H^+ + SO_4^{2-} = CaHSO_4^+$ | 2.40‡ |
| $Cu^{2+} + H_2O - H^+ = CuOH^+$ | −8.17‡ |
| $Cu^{2+} + 2H_2O - 2H^+ = Cu(OH)_2^0$ | −13.8‡ |
| $Cu^{2+} + 3H_2O - 3H^+ = Cu(OH)_3^-$ | −26.9‡ |
| $Cu^{2+} + 4H_2O - 4H^+ = Cu(OH)_4^{2-}$ | −39.3‡ |
| $Cu^{2+} + SO_4^{2-} = CuSO_4^0$ | 1.59 |
| $Fe^{2+} + H_2O - H^+ = FeOH^+$ | −10.3 |
| $Fe^{2+} + 2H_2O - 2H^+ = Fe(OH)_2^0$ | −22.2 |
| $Fe^{2+} + SO_4^{2-} = FeSO_4^0$ | 4.14 |
| $Fe^{2+} + H^+ + SO_4^{2-} = FeHSO^+$ | 2.40‡ |
| $Fe^{3+} + H_2O - H^+ = FeOH^{2+}$ | −3.08 |
| $Fe^{3+} + 2H_2O - 2H^+ = Fe(OH)_2^+$ | −7.07 |
| $Fe^{3+} + 3H_2O - 3H^+ = Fe(OH)_3^0$ | −15.5 |
| $Fe^{3+} + 4H_2O - 4H^+ = Fe(OH)_4^-$ | −23.6 |
| $Fe^{3+} + SO_4^{2-} = FeSO_4^+$ | 2.83 |
| $Fe^{3+} + H^+ + SO_4^{2-} = FeHSO_4^{2+}$ | 3.64‡ |
| $Fe^{3+} + 2SO_4^{2-} = Fe(SO_4)_2^-$ | 3.84 |
| $Al^{3+} + H_2O - H^+ = AlOH^{2+}$ | −5.93 |
| $Al^{3+} + 2H_2O - 2H^+ = Al(OH)_2^+$ | −12.0 |
| $Al^{3+} + 3H_2O - 3H^+ = Al(OH)_3^0$ | −19.5 |
| $Al^{3+} + 4H_2O - 4H^+ = Al(OH)_4^-$ | −25.2 |
| $Al^{3+} + SO_4^{2-} = AlSO_4^+$ | 1.90 |
| $Al^{3+} + H^+ + SO_4^{2-} = AlHSO_4^{2+}$ | 1.62‡ |
| $Al^{3+} + 2SO_4^{2-} = Al(SO_4)_2^-$ | 3.47 |
| **Solid phases and surface complexes** | |
| $Fe(OH)_3(s) = Fe^{3+} + 3H_2O - 3H^+$ | 5.39‡ |
| $Al_2Si_2O_5(OH)_4(s)$ $= 2Al^{3+} + 2H_4SiO_4^0 + H_2O - 6H^+$ | 10.3 |
| $SiO_2(s) = H_4SiO_4^0 - 2H_2O$ | −3.37 |
| $>FeOH + H^+ = >FeOH_2^+$ | 6.45§ |
| $>FeOH = >FeO^- + H^+$ | −8.27§ |
| $>FeOH + Fe^{2+} = >FeOFe^+ + H^+$ | −1.99§ |
| $>FeOH + Fe^{2+} + H_2O = >FeOFeOH + 2H^+$ | −8.39§ |
| **Gas phase** | |
| $O_2(g) = O_2(aq)$ | −2.68‖ |

*Components used in the model are $H^+$, $Na^+$, $K^+$, $Mg^{2+}$, $Ca^{2+}$, $SO_4^{2-}$, $Fe^{2+}$, $Cu^{2+}$, >FeOH, $SiO_2(s)$, $O_2(aq)$, $Fe(OH)_3(s)$ for Fe(III) and $Al_2Si_2O_5(OH)_4(s)$ for Al.

†The given conditional stability constants were calculated for a temperature correction to 278 K with the van't Hoff equation and an ionic strength correction to $I = 0.05$ M with the Davies equation. Stability constants were taken from the WATEQ database (Truesdell and Jones, 1974) revised by Nordstrom *et al.* (1991), if not otherwise stated.

‡$\Delta H^0$ not available.

§Zhang *et al.* (1994), electrostatic and temperature corrections have not been considered.

‖Solubility of $O_2(aq)$ at 278 K from Stumm and Morgan (1981), $K$(M/atm).

ing of primary minerals (processes 6–10) are valid for surface-reaction controlled dissolution kinetics. The fractional-order dependence on dissolved proton concentration is related to the concentration of reactive surface hydrolysis species (Grauer and Stumm, 1982; Blum and Lasaga, 1988). The acceleration and inhibition of the dissolution reactions due to changes in surface hydrolysis speciation with pH are therefore implicitly accounted for in these fractional order empirical rate laws (Wieland *et al.*, 1988). Inhibition and acceleration of reaction kinetics due to other surface reactants such as adsorbed metal ions are not included.

All sulphide minerals are far from equilibrium in oxic environments, and weathering rates are constrained only by reaction kinetics and transport of molecular oxygen. Because the heaps have remained oxic, we do not expect the thermodynamic stability of the different sulphides to have an influence on dissolution rates. For abiotic pyrite oxidation by dissolved oxygen (process 3), numerous studies on reaction rates have been published (e.g. Clark, 1966; Mathews and Robins, 1974; Goldhaber, 1983; Moses *et al.*, 1987). Experiments by Smith *et al.* (1968) and McKibben and Barnes (1986) suggest a low reaction rate dependence on free proton concentration, $[H^+]^{-0.1}$, which we considered insignificant in comparison with field-scale uncertainties. Rate dependence on concentration of dissolved oxygen has been found to fit a Langmuir adsorption isotherm (Nicholson *et al.*, 1988), which can be approximated as a fractional order dependence. Here we use a square root dependence (McKibben and Barnes, 1986). The rate constant, $k_{pyo}$, was calibrated to recent compilations of pyrite reaction rates (Williamson, 1992, R. V. Nicholson, pers. comm. 1992), obtained by comparison of independent experimental investigations (e.g. McKay and Halpern, 1958; McKibben and Barnes, 1986; Nicholson *et al.*, 1988; Moses and Herman, 1991). The reaction rate of 25°C, pH 2–8, and $pO_2 = 0.21$ atm was found to be $5 \pm 3 \times 10^{-10}$ mol/m$^2$ s.

The relative importance of pyrite oxidation by ferric iron has been investigated and debated (Garrels and Thompson, 1960; Nebgen *et al.*, 1981; McKibben and Barnes, 1986). This reaction (process 4) has been referred to as the indirect mechanism (Silverman, 1967) and is here formulated as consumption of Fe(III) hydroxide. For the sake of simplicity we use the rate law suggested by Wiersma and Rimstidt (1984), which is first order with respect to the concentration of $Fe^{3+}$. Although no published rate law covers a wide pH range, the reaction has been shown to dominate at pH 1.6 (Herrera *et al.*, 1989), and is inhibited at neutral pH due to competitive adsorption of Fe(II) (Moses and Herman, 1991). The indirect mechanism has also been shown to be less important in unsaturated hydrological environments and for conditions of high iron oxidizing microbial activity (Taylor *et al.*, 1984a,b).

Table 4. Stoichiometry of processes*

(1) Inflow of atmospheric precipitation:

$\rightarrow 2H^+ + SO_4^{2-}$

(2) Ferrous iron oxidation:

$Fe^{2+} + \frac{1}{4}O_2(aq) + \frac{5}{2}H_2O \rightarrow Fe(OH)_3(s) + 2H^+$

(3) Pyrite oxidation by dissolved oxygen:

$FeS_2(s) + \frac{7}{2}O_2(aq) + H_2O \rightarrow Fe^{2+} + 2SO_4^{2-} + 2H^+$

(4) Pyrite oxidation by ferric iron:

$FeS_2(s) + 14Fe(OH)_3(s) + 26H^+ \rightarrow 15Fe^{2+} + 2SO_4^{2-} + 34H_20$

(5) Chalcopyrite oxidation by dissolved oxygen:

$CuFeS_2(s) + 4O_2(aq) \rightarrow Cu^{2+} + Fe^{2+} + 2SO_4^{2-}$

(6) Muscovite dissolution:

$KAl_2[AlSi_3O_{10}](OH)_2(s) + H^+ + \frac{3}{2}H_2O \rightarrow K^+ + \frac{3}{2}Al_2Si_2O_5(OH)_4(s)$

(7) Biotite dissolution:

$KMg_{1.5}Fe_{1.5}AlSi_3O_{10}(OH)_2(s) + 7H^+ + \frac{1}{2}H_2O \rightarrow K^+ + 1.5Mg^{2+} + 1.5Fe^{2+} + 2H_4SiO_4^0 + \frac{1}{2}Al_2Si_2O_5(OH)_4(s)$

(8) Albite dissolution:

$NaAlSi_3O_8(s) + H^+ + \frac{9}{2}H_2O \rightarrow Na^+ + 2H_4SiO_4^0 + \frac{1}{2}Al_2Si_2O_5(OH)_4(s)$

(9) Anorthite dissolution:

$CaAl_2Si_2O_8(s) + 2H^+ + H_2O \rightarrow Ca^{2+} + Al_2Si_2O_5(OH)_4(s)$

(10) K-feldspar dissolution:

$KAlSi_3O_8(s) + H^+ + \frac{9}{2}H_2O \rightarrow K^+ + 2H_4SiO_4^0 + \frac{1}{2}Al_2Si_2O_5(OH)_4(s)$

(11) Outflow

All aqueous species in reactor $\rightarrow$

*The stoichiometry of processes are inserted in the STEADYQL program as congruent reactions. The activity of Fe(III), $H_4SiO_4$ and Al in solution are then controlled by the solubility of $Fe(OH)_3$(s), $SiO_2$(s) and $Al_2Si_2O_5(OH)_4$(s). Stoichiometries of dominating processes are shown in the table.

Table 5. Expressions for processes*

| Process | | Ref. |
|---|---|---|
| 1 | $J_{in} = qc_{in}$ | |
| 2 | $J_{feo} = h\theta[O_2(aq)](k_{fe1}[Fe^{2+}] + k_{fe2}[Fe(OH)^+] + k_{fe3}[>FeOFe^+])$ | (1) |
| 3 | $J_{pyo} = hA_{py}k_{pyo}[O_2(aq)]^{0.5}$ | (2) |
| 4 | $J_{pyf} = hA_{py}k_{pyf}[Fe^{3+}]$ | (3) |
| 5 | $J_{cho} = hA_{ch}k_{cho}[O_2(aq)]^{0.5}$ | † |
| 6 | $J_{mud} = hA_{mu}(k_{mu1}[H^+]^{0.4} + k_{mu2})$ | (4) |
| 7 | $J_{bld} = hA_{bl}k_{bld}[H^+]^{0.6}$ | (5) |
| 8 | $J_{ald} = hA_{al}k_{ald}[H^+]^{0.4}$ | (6) |
| 9 | $J_{and} = hA_{an}(k_{an1}[H^+]^{2.7} + k_{an2})$ | (7) |
| 10 | $J_{kfd} = hA_{kf}k_{kfd}$ | (8) |
| 11 | $J_{out} = qc^i_{out}$ | ‡ |

*Parameters: $q$ = infiltration rate (m/s); $h$ = height of heap (m); $\theta$ = water content ($m^3/m^3$ of media); $A_i$ = surface area of mineral ($m^2/m^3$ of media); $k_i$ = rate constant, units according to Table 6; $J_i$ = flux per heap area (mol/$m^2$/s).

†Reaction rate of chalcopyrite was assumed to depend on $PO_2$ in the same way as pyrite.

‡Outflow, $J_{out}$ calculated by program (mol/ha/a).

References: (1) Wehrli (1990); (2) McKibben and Barnes (1986); (3) Wiersma and Rimstidt (1984); (4) Knauss and Wolery (1989); (5) Malmström and Banwart (in preparation); (6) Chou and Wollast (1985); (7) Amrhein and Suarez (1988); (8) Helgeson *et al.* (1984).

We are aware of only one published study of chalcopyrite oxidation (process 5). In a comparison of the oxidative dissolution of chalcopyrite and pyrite in batch reactors open to the atmosphere, the rate of the chalcopyrite reaction was approximately half that of pyrite (Steger and Desjardins, 1978). It was not possible with the information presented to normalize the relative reaction rates to specific surface area. As

Table 6. Parameters in processes

| Process | Parameter* | Ref. |
|---|---|---|
| 1 | $q = 1.6 \times 10^{-8}$ (m/s) | |
| 1 | $c_{in} = 6.3 \times 10^{-6}$ (M) | |
| 2–11 | $h = 15$ (m) | |
| 2, 3, 5 | $PO_2 = 0.10$ (atm) | |
| 2 | $k_{fe1} = 4.8 \times 10^{-9}$ ($m^3$/mol/s/) | (1)† |
| 2 | $k_{fe2} = 15.3 \times 10^{-3}$ ($m^3$/mol/s) | (1) |
| 2 | $k_{fe3} = 2.8 \times 10^{-3}$ ($m^3$/mol/s) | (1) |
| 2 | $T = 1 \times 10^{-3}$ (M) | ‡ |
| 2 | $\theta = 0.05$ | |
| 3 | $k_{pyo} = 7.9 \times 10^{-11}$ ($mole^{0.5}$ $m^{1.5}/m^2/s$) | (2) |
| 4 | $k_{pyf} = 1.3 \times 10^{-9}$ ($m^3/m^2/s$) | (3) |
| 5 | $k_{cho} = 4.1 \times 10^{-11}$ ($mol^{0.5}$ $m^{1.5}/m^2/s$) | § |
| 6 | $k_{mu1} = 9.5 \times 10^{-15}$ ($mol^{0.6}$ $m^{1.2}/m^2/s$) | (4) |
| 6 | $k_{mu2} = 1.8 \times 10^{-15}$ ($mol/m^2/s$) | (4) |
| 7 | $k_{bld} = 7.8 \times 10^{-12}$ ($mole^{0.4}$ $m^{1.8}/m^2/s$) | (5) |
| 8 | $k_{ald} = 3.3 \times 10^{-12}$ ($mole^{0.6}$ $m^{1.2}/m^2/s$) | (6) |
| 9 | $k_{an1} = 7.9 \times 10^{-10}$ ($mole^{-1.7}$ $m^{8.1}/m^2/s$) | (7) |
| 9 | $k_{an2} = 4.6 \times 10^{-13}$ ($mol/m^2/s$) | (7) |
| 10 | $k_{kfd} = 4.1 \times 10^{-13}$ ($mol/m^2/s$) | (8) |

*Rate constants are corrected to 278 K with the Arrenius expression.

†The influence of temperature on process 2 is considered by correcting for the temperature-dependent solubility of oxygen and ion product of water (Sung and Morgan, 1980).

‡Total concentration of immobiles sites, (M).

§The rate of chalopyrite oxidation was assumed to be half that of pyrite as indicated by experimental results of Steger and Desjardins (1978).

References: (1) Wehrli (1990); (2) Williamson (1992); (3) Wiersma and Rimstidt (1984); (4) Knauss and Wolery (1989); (5) Malmström and Banwart (in preparation); (6) Chou and Wollast (1985); (7) Amrhein and Suarez (1988); (8) Helgeson *et al.* (1984).

Table 7. Total concentrations of dominating elements in leachate (mM), collected in drainage ditch D1 (Fig. 1) and results of corresponding simulations with abiotic sulphide weathering rate from literature and with a calibrated sulphide weathering rate

| | Field data | Model Abiotic sulphide rate | Model Calibrated sulphide rate* |
|---|---|---|---|
| pH | 3.80 | 4.1 | 3.8 |
| Cu | 0.30 | 0.5 | 0.5 |
| Fe | 0.04 | 0.02 | 0.09 |
| Al | 2.8 | 0.3 | 3 |
| Ca | 4.6 | 1 | 3 |
| Mg | 2.4 | 5 | 3 |
| Na | 2.0 | 4 | 2 |
| K | 0.44 | 6 | 3 |
| $SO_4$ | 13.6 | 13 | 14 |
| Si | 0.32 | 0.4 | 0.4 |
| Ionic strength, $I$ (M) | 0.038 | 0.04 | 0.04 |
| $A_{r,tot}$($m^2/m^3$) | – | $3 \times 10^4$ | $1.1 \times 10^4$ |

*($k'_{pyo}$, $k'_{pyf}$, $k'_{cho}$) = 3 × ($k_{pyo}$, $k_{pyf}$, $k_{cho}$).

no explicit rate law has been given in the literature, the rate dependence on $O_2$(aq) and free proton concentration for chalcopyrite dissolution was assumed to be the same as for pyrite. Chalcopyrite oxidation by ferric iron was assumed to be negligible.

All sulphide oxidation reactions (processes 3–5) only consider complete oxidation to sulphate. Although elemental sulphur and aqueous species of intermediate redox state ($S_4O_6^{2-}$, $S_2O_3^{2-}$, $SO_3^{2-}$) may also form, experimental results show that sulphate is dominating (Steger and Desjardins, 1978; McKibben and Barnes, 1986; Moses *et al.*, 1987; Moses and Herman, 1991). Microbially mediated reaction kinetics were not explicitly evaluated but were considered by comparison with modelled abiotic reaction rates as discussed below.

### *Reactive and physical surface area*

The reactive surface area of the waste rock, $A_{r,tot}$ ($m^2/m^3$ of media), was treated as a dependent variable, calibrated to arrive at a leachate of an ionic strength that corresponds to site measurements. The reactive surface area for a specific mineral $A_i$, is assumed to be related to mineral volume abundance $v_i$, and the calibrated total reactive surface area, $A_{r,tot}$, as shown below. Differences in grain sizes and surface roughness between different minerals which could effect the distribution of surface area were neglected:

$$X_i = \frac{v_i}{\sum_{j=1}^{n} v_j} \tag{6}$$

$$A_i = X_i A_{r,tot} (m^2/m^3 \text{ of media}). \tag{7}$$

A "physical" surface area of the waste rock was estimated at BET surface area, using $N_2$(g) sorption (Micromeritics, Flow sorb II 2300). Particles of the different rock types and different size fractions (diameter; 0.1, 0.2, 0.3, 0.7, 1.4, 2.8, 4.7 mm) were ultrasonically cleaned before measurements. Results show an average surface area of 1 ± 0.4 $m^2/g$. No significant difference between different rock types or particle size fractions could be detected. The measured specific surface is much greater than the geometrical outer surface area of the particles, presumably due to inner pore surfaces. The outer geometric surface area only becomes important for comparatively small fraction of particles with diameters below 10 $\mu$m (assuming spherical geometry). It could thus be concluded that physical surface area is approximately constant per volume rock and independent of the particle size distribution. At an estimated density for the waste rock at 2800 $kg/m^3$ and an assumed porosity for the heaps of 35%, the physical surface area is of the order of $2 \times 10^6$ $m^2/m^3$.

## RESULTS AND DISCUSSION

The model calculations give a leachate with composition shown in Table 7 (column 2). The comparison with the average leachate composition measured

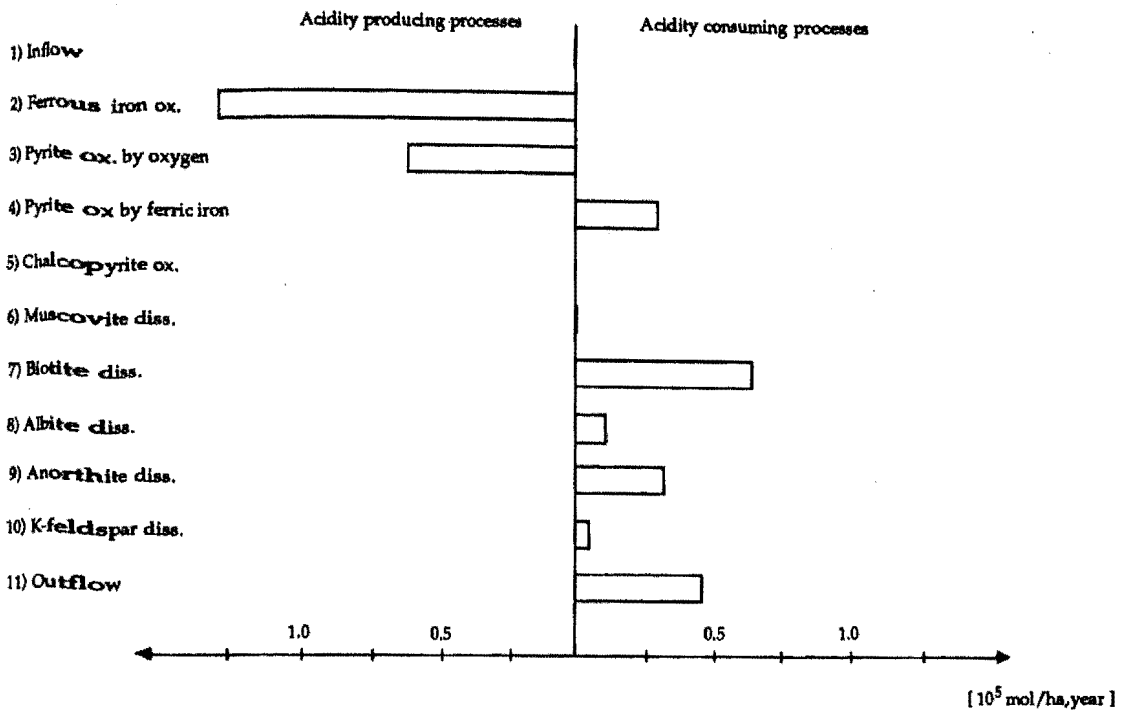


FIG. 3. Proton balance of steady-state model for geochemical processes at the site ($10^5$ mol/ha/a). Acidity is defined as the base neutralizing capacity [BNC, Eqn (1)].

at the site (column 1) shows that the *relative* rate of sulphide mineral weathering and alkalinity generation from dissolution of primary silicate minerals explains the net proton flux at the site reasonably well. Because the dominant process driving all reactions at this site is the sulphide oxidation, the sulphide reaction rates ($k_{pyf}$, $k_{pyo}$, $k_{cho}$) were increased by a factor of 3 to give the same pH as the site drainage water. The results for all components agreed significantly better after this relatively small adjustment (column 3, Table 7). This difference in reaction rate is of the same order of magnitude as uncertainties in measured flowrates and the chemical composition of water in the drainage ditches.

Concerning microbial catalysis, *Thiobacillus ferrooxidans* has been reported to increase weathering rates of pyrite more than one order of magnitude in laboratory experiments under optimal growth conditions (PACIOREK *et al.*, 1981; LIZAMA and SUZUKI, 1989; OLSON, 1991). The activity of these acidophilic bacteria increases with decreasing pH below pH 4 (ARKESTEYN, 1980) with optimal growth conditions observed at temperatures near 30°C (SILVERMAN and LUNDGREN, 1959). Porewater pH at this site is within the reported pH range for *Thiobacillus ferrooxidans* activity. However, their activity may be restricted by the low average temperature at this site. The deviation in sulphide reaction rates by a factor of three from abiotic kinetic data can be considered small and is not necessarily related to bacterial sulphide oxidation.

Comparison of Fe(II) production from pyrite and biotite weathering with Fe fluxes in the drainage water shows that at least 99% of iron is removed within the waste rock heap. This internal cycling could only be explained by a rate of Fe(II) oxidation which is three orders-of-magnitude faster than that predicted by the abiotic rate of reaction. The abiotic reaction was dominated by the surface-catalysed pathway. Consistent model results could only be obtained when this reaction rate was explicitly corrected to account for the large discrepancy in reaction rates. Microbially-catalysed ferrous iron oxidation by *Thiobacillus ferrooxidans* or other iron-oxidizing bacteria (NIKOLOV and KARAMANEV, 1992; AHONEN and TUOVINEN, 1989) must therefore be considered. The rate of sulphate and base cation production from mineral dissolution and the corresponding element fluxes in the site drainage water indicate that iron is removed predominantly as Fe(III) hydroxide rather than as mixed hydroxy–sulphate phases such as jarosite.

The *relative* reaction rate of silicate minerals explains measured fluxes of base cations; $K^+$, $Mg^{2+}$, $Na^+$, $Ca^{2+}$. Reaction rates of pure silicate minerals measured in laboratory experiments often vary depending on differences in mineral composition, surface morphology and experimental method. In spite of these uncertainties, the correlation between model results and field measurement show that the relative reactivity observed in the field is consistent with the laboratory results.

The model calculations show a proton balance (Fig. 3) with alkalinity production dominated by the

Table 8. Characteristic turnover time of minerals and rate constants for mineral dissolution

| | Turnover time* (a) | Rate constant† (mol/m²/s) |
|---|---|---|
| Pyrite | 700 | $6 \times 10^{-13}$ |
| Chalcopyrite | 800 | $2 \times 10^{-13}$ |
| Anorthite | $3 \times 10^3$ | $4 \times 10^{-14}$ |
| Biotite | $5 \times 10^3$ | $1 \times 10^{-14}$ |
| Albite | $1 \times 10^4$ | $1 \times 10^{-14}$ |
| K-feldspar | $4 \times 10^4$ | — |
| Muscovite | $3 \times 10^6$ | — |

*Determined from mineral content of waste rock heap and weathering calculated by the steady-state model.

†Rate constants obtained from element fluxes at the site and normalized to a measured (BET) mineral surface area. Tracers: $Cu^{2+}$, chalcopyrite; $SO_4^{2-}$ (corrected for chalcopyrite oxidation), pyrite; $Ca^{2+}$, anorthite; $Na^+$, albite; $Mg^{2+}$, biotite.

weathering of biotite and anorthite. It is interesting to note that this is consistent with conclusions drawn from watershed studies showing either plagioclase (KIRKWOOD and NESBITT, 1991) or ferromagnesian silicates (MILLER and DREVER, 1977) or both (GIOVANOLI *et al.*, 1988; VELBEL, 1985) as dominating sources of alkalinity. Acidity generation is dominated by ferrous iron oxidation to Fe(II) hydroxide and oxidative weathering of pyrite.

The *absolute* weathering rates in the waste rock heaps are affected by the fraction of the mineral surface area accessible for reaction with porewater. A significant part of inner pore surfaces may be inaccessible due to a low transport rate of dissolved reactants within particles. The reactive surface area used to obtain model results, $1.1 \times 10^4$ ($m^2/m^3$ of media), compares to an estimated physical surface area of $2 \times 10^6$ ($m^2/m^3$ of media), obtained from the BET measurements of waste rock particles. This corresponds to a reactive surface area of 0.6% of physical surface area which is a similar level as for a number of other field systems (WHITE and PETERSON, 1990).

It should be noted that field effects not directly related to the reactive surface area, for example adsorption of dissolution inhibiting ions such as aluminium and sulphate or transport controlled reaction rates (SCHNOOR, 1990; STUMM, 1991), may effect its calibration. Nonetheless, we consider the calibration of reactive surface area the only feasible approach to such uncertainties with the present knowledge of field-scale processes.

Dissolution rates were also calculated directly from element fluxes at the site, and normalized to the physical surface area, using $Mg^{2+}$ as a tracer for biotite, $Na^+$ for albite, $Ca^{2+}$ for anorthite, $Cu^{2+}$ for chalcopyrite and $SO_4^{2-}$ for pyrite (corrected for chalcopyrite weathering; Table 8). As in the model development, other sources or internal sinks for the elements are neglected. Neglecting dissolution of trace amounts of calcite and a possible precipitation of gypsum may alter the given weathering rates for anorthite and pyrite. However, because the calcite dissolution has been demonstrated to be significant only for a time scale shorter than the average age of the heaps (STRÖMBERG *et al.*, 1994), we do not expect significant $Ca^{2+}$ generation from calcite dissolution here. In general, directly calculating weathering rates by these element fluxes at field scale is justified considering the relatively good agreement between model results and net proton flux at the site.

We calculated a characteristic turnover time for each mineral (Table 8) by dividing the total amount of mineral in the heaps by their respective dissolution rates at steady state. Because geochemical processes controlling dissolution rates may change significantly over geological time scales, these characteristic times are not necessarily related to the lifetime of the minerals. However, these turnover times can be compared with the estimated hydraulic residence time of 1.5 a. For the elements included as components in the model calculations above; $Na^+$, $K^+$, $Mg^{2+}$, $Ca^{2+}$, $Cu^{2+}$, $SO_4^{2-}$, are considered conservative solutes whose turnover time is of the same order as the hydraulic residence time. On the other hand, elements dominated by internal cycling (participate in secondary mineral formation); $H^+$, $Fe^{2+}$, $Fe^{3+}$, $Al^{3+}$, $H_4SiO_4(aq)$, $O_2(aq)$, have turnover times on the order of days. This comparison provides a justification for the steady-state model, as changes in the relative mineral abundance are slow compared to the residence times of solutes. On time scales greater than $10^1$–$10^2$ a, those changes must be considered.

## CONCLUSIONS

Considering uncertainty in drainage water flow and composition at the site, treating the waste rock heap as a single completely-mixed reactor is an appropriate level of complexity for coupled chemical and hydrological processes. In spite of neglecting spatial and temporal variability in mineral composition, weathering rates and hydrologic conditions, we can conclude the following.

(1) The *relative* weathering rates of sulphides and primary silicate minerals taken from the literature, explain net proton and base cation fluxes at the site.

(2) The overall rate of $Fe^{2+}$ oxidation within the heap is at least three orders of magnitude faster than that given by abiotic kinetics. The activity of iron oxidizing bacteria should therefore be considered.

(3) The *absolute* weathering rates, normalized to a physical surface area estimated by BET measurements and with activation energies corrected for temperature, are approximately two orders of magnitude lower at field scale compared to published rates from laboratory experiments.

(4) Drainage water concentrations indicate that Si, Al and $Fe^{3+}$ flux is controlled by solubility equilibrium with secondary minerals and flow rate through

the heap, whereas reaction kinetics influence release rates of acidity, $SO_4$, Cu, base cations and possibly $Fe^{2+}$.

(5) Model calculations indicate that weathering of biotite and plagioclase are dominant sources of alkalinity.

*Acknowledgements*—R. J. Bowell and R. Raiswell are gratefully acknowledged for helpful review comments. We also thank A. I. M. Ritchie for valuable discussions during his visit in Stockholm. This study would not have been possible without Hans Jönsson, Boliden Mineral AB, who provided information about the site, mineralogical data and most of the chemical analyses. Funding was received from the von Kantzow foundation and the Swedish Waste Research Council.

*Editorial handling*: Mike Edmunds.

## REFERENCES

AHONEN L. and TUOVINEN O. H. (1989) Microbiological oxidation of ferrous iron at low temperatures. *Appl. Environ. Microbiol.* **55**, 312–316.

ALPERS C. N., NORDSTROM D. K. and BALL J. W. (1989) Solubility of jarosite solid solutions precipitated from acid mine waters, Iron Mountain, California, U.S.A. *Sci. Geol. Bull.* **42**, 281–298.

AMRHEIN C. and SUAREZ D. L. (1988) The use of a surface complexation model to describe the kinetics of ligand-promoted dissolution of anorthite. *Geochim. cosmochim. Acta* **52**, 2785–2793.

ARKESTEYN G. J. M. W. (1980) Pyrite oxidation in acid sulphate soils: The role of microorganisms. *Plant & Soil* **54**, 119–134.

AXELSSON C. L., BYSTRÖM J., HOLMÉN J. and JANSSON T. (1992) Efterbehandling av sandmagasin och gråbergsupplag i Aitik, Hydrogeologiska förutsättningar för åtgärdsplan. Report 927-1801, Golder Geosystem AB (in Swedish).

BARTLETT R. W. (1992) Simulation of ore heap leaching using deterministic models. *Hydrometallurgy* **29**, 231–260.

BENNETT J. W., GIBSON D. K., PANTELIS G., RITCHIE A. I. M. and TAN Y. (1992) Pyritic oxidation mechanisms and pollution loads at the Aitik mine site; Assessment after first ten months monitoring. ANSTO/C262.

BENNETT J. W. and RITCHIE A. I. M. (1991) Measurements of the transport of oxygen into two rehabilitated waste rock dumps. In *Second International Conference on the Abatement of Acidic Drainage, Montreal*, pp. 289–298.

BERGSTRÖM U. (1981) Mineralogisk undersökning av generalprov från Aitik, Boliden Mineral AB, GCM/AIM/26/81 (in Swedish).

BERGSTRÖM U. (1982) Mineralogisk undersökning av generalprov från Aitik, nivå 100–250 m. Boliden Mineral AB, GCM/AIM/28/82 (in Swedish).

BLOWES D. W., REARDON E. J., JAMBOR J. L. and CHERRY J. A. (1991) The formation and potential importance of cemented layers in inactive sulfide mine tailings. *Geochim. cosmochim. Acta* **55**, 965–978.

BLUM A. and LASAGA A. (1988) Role of surface speciation on the low temperature dissolution of minerals. *Nature* **331**, 431.

CATHLES L. M. and APPS J. A. (1975) A model of the dump leaching process that incorporates oxygen balance, heat balance and air convection. *Metall. Trans.* **6B**, 617–624.

CHOU L. and WOLLAST R. (1985) Steady-state kinetics and dissolution mechanisms of albite. *Am. J. Sci.* **285**, 963–993.

CLARK C. S. (1966) Oxidation of coal mine pyrite. *J. Sanit. Eng. Div. Am. Soc. Civ. Engrs* **92**, 127–145.

DAVIS G. B. and RITCHIE A. I. M. (1986) A model of oxidation in pyritic mine wastes: part 1 equations and approximate solution. *Appl. Math. Modell.* **10**, 314–322.

DIXON D. G. and HENDRIX J. L. (1993) A general model for leaching of one or more solid reactants from porous ore particles. *Metall. Trans.* **24B**, 157–169.

FURRER G., SOLLINS P. and WESTALL J. (1990) The study of soil chemistry through quasi-steady-state models: II Acidity of soil solution. *Geochim. cosmochim. Acta* **54**, 2363–2374.

FURRER G., WESTALL J. and SOLLINS P. (1989) The study of soil chemistry through quasi-steady-state models: I Mathematical definition of problem. *Geochim. cosmochim. Acta* **53**, 595–601.

GARRELS R. M. and THOMPSON M. E. (1960) Oxidation of pyrite by iron sulfate solutions. *Am. J. Sci.* **258-A**, 57–67.

GÉLINAS P., LEFEBVRE R. and CHOQUETTE M. (1992) Monitoring of acid mine drainage in a waste rock dump. In *Environmental Issues and Management of Waste in Energy and Mineral Production, Vol.* 2 (eds R. K. SINGHAL, A. K. MEHROTRA, K. FYTAS and J. L. COLLINS), pp. 747–756. Balkema, Rotterdam.

GIOVANOLI R., SCHNOOR J. L., SIGG L., STUMM W. and ZOBRIST J. (1988) Chemical weathering of crystalline rocks in the catchment area of acidic Ticino Lakes, Switzerland. *Clays Clay Miner.* **36**, 521–529.

GOLDHABER M. B. (1983) Experimental study of metastable sulfur oxyanion formation during pyrite oxidation at pH 6–9 and 30°C. *Am. J. Sci.* **283**, 193–217.

GRAUER R. and STUMM W. (1982) Die koordinationschemie oxidischer grenzflächen und ihre auswirkung auf die auflösungsuskinetic oxidischer festphasen in wässerig lösungen. *Colloid Polymer Sci.* **260**, 959.

HARRIES J. R. and RITCHIE A. I. M. (1981) The use of temperature profiles to estimate the pyritic oxidation rate in a waste rock dump from an opencut mine. *Water Air Soil Pollut.* **15**, 405–423.

HARRIES J. R. and RITCHIE A. I. M. (1985) Pore gas composition in waste rock dumps undergoing pyritic oxidation. *Soil Sci.* **140**, 143–152.

HELGESON H. C. (1968) Revaluation of irreversible reactions in geochemical processes involving minerals and aqueous solutions—I. Thermodynamic relations. *Geochim. cosmochim. Acta* **32**, 853–877.

HELGESON H. C. (1979) Mass transfer among minerals and hydrothermal solutions. In *Geochemistry of Hydrothermal Ore Deposits* (ed. H. L. BARNES), Chap. 11, pp. 568–610. J. Wiley & Sons, Chichester.

HELGESON H. C., GARRELS R. M. and MACKENZIE F. T. (1969) Evaluation of irreversible reactions in geochemical processes involving minerals and aqueous solutions—II. Applications. *Geochim. cosmochim. Acta* **33**, 455–481.

HELGESON H. C., MURPHY W. M. and AAGAARD P. (1984) Thermodynamic and kinetic constraints on reaction rates among minerals and aqueous solutions. II. Rate constants, effective surface area, and the hydrolysis of feldspar. *Geochim. cosmochim. Acta* **48**, 2405–2432.

HERRERA M. N., WIERTZ J. V., RUIZ P., NEUBURG H. J. and BADILLA-OHLBAUM R. (1989) A phenomenological model of the bioleaching of complex sulfide ores. *Hydrometallurgy* **22**, 193–206.

HOLLAND H. D., LAZAR B. and MCCAFFREY M. (1986) Evolution of the atmosphere and the oceans. *Nature* **320**, 27–33.

KARLSSON S., ALLARD B. and HÅKANSSON K. (1988) Characterization of suspended solids in a stream receiving acid mine effluents, Bersbo, Sweden. *Appl. Geochem.* **3**, 345–356.

KIRKWOOD D. E. and NESBITT H. W. (1991) Formation and evolution of soils from an acidified watershed: Plastic Lake, Ontario, Canada. *Geochim. cosmochim. Acta* **55**, 1295–1308.

KNAUSS K. G. and WOLERY T. J. (1989) Muscovite dissolution kinetics as a function of pH and time at 70°C. *Geochim. cosmochim. Acta* **53**, 1493–1501.

LARSSON R. (1992) Aitik—kvantiteter och halter av brutet gråberg. Boliden Mineral AB, Gruvgeologirapport nr 368 (in Swedish).

LASAGA A. C. (1984) Chemical kinetics of water–rock interactions. *J. geophys. Res.* **89**, 4009–4025.

LEVENSPIEL O. (1972) *Chemical Reaction Engineering*. John Wiley & Sons, Chichester.

LIZAMA H. M. and SUZUKI I. (1989) Rate equations and kinetic parameters of the reactions involved in pyrite oxidation by *Thiobacillus ferrooxidans*. *Appl. Environ. Microbiol.* **55**, 2918–2923.

MATHEWS C. T. and ROBINS R. G. (1974) Aqueous oxidation of iron disulphide by molecular oxygen. *Aust. Chem. Eng.* (Nov–Dec) **21**, 19–24.

MCKAY D. R. and HALPERN J. (1958) A kinetic study of the oxidation of pyrite in aqueous suspension. *Trans. Metall. Soc. AIME* **212**, 301–309.

MCKIBBEN M. A. and BARNES H. L. (1986) Oxidation of pyrite in low temperature acidic solutions: Rate laws and surface textures. *Geochim. cosmochim. Acta* **50**, 1509–1520.

MILLER W. R. and DREVER J. I. (1977) Chemical weathering and related controls on surface water chemistry in the Absaroka Mountains, Wyoming. *Geochim. cosmochim. Acta* **41**, 1693–1702.

MOSES C. O. and HERMAN J. S. (1991) Pyrite oxidation at circumneutral pH. *Geochim. cosmochim. Acta* **55**, 471–482.

MOSES C. O., NORDSTROM D. K., HERMAN J. S. and MILLS A. L. (1987) Aqueous pyrite oxidation by dissolved oxygen and by ferric iron. *Geochim. cosmochim. Acta* **51**, 1561–1571.

NEBGEN J. W., ENGELMAN W. H. and WEATHERMAN D. F. (1981) Inhibition of acid mine drainage formation: The role of insoluble iron compounds. *J. Environ. Sci.* **24**,(3), 23–27.

NICHOLSON R. V., GILLHAM R. V. and REARDON E. J. (1988) Pyrite oxidation in carbonate-buffered solutions: 1. Experimental kinetics. *Geochim cosmochim. Acta* **52**, 1077–1085.

NIKOLOV L. N. and KARAMANEV D. G. (1992) Kinetics of the ferrous iron oxidation by resuspended cells of *Thiobacillus ferrooxidans*. *Biotechnol. Prog.* **8**, 252–255.

NORDSTROM D. K., JENNE E. A. and BALL J. W. (1979) Redox equilibria of iron in acid mine waters. In *Chemical Modeling of Aqueous Systems* (ed. E. A. JENNE), Chap 3, pp. 51–79. ACS Symposium Series 93.

NORDSTROM D. K., PLUMMER L. N., LANGMUIR D., BUSENBERG E., MAY H. M., JONES B. F. and PARKHURST D. L. (1991) Revised chemical equilibrium data for major water–mineral reactions and their limitations. In *Chemical Modeling of Aqueous Systems II* (eds D. C. MELCHOIR and R. L. BASSETT), Chap 31, pp. 398–413. ACS Symposium Series 416.

OLSON G. J. (1991) Rate of pyrite bioleaching by *Thiobacillus ferrooxidans*: results of an interlaboratory comparison. *Appl. Environ. Microbiol.* **57**, 642–644.

PACIOREK K. J. L., KRATZER R. H., KIMBLE P. F., TOBEN W. A. and VATASESCU A. L. (1981) Degradation of massive pyrite: physical, chemical and bacterial effects. *Geomicrobiol. J.* **2**, 363–375.

PANTELIS G. and RITCHIE A. I. M. (1991) Macroscopic transport mechanisms as a ratelimiting factor in dump leaching of pyritic ores. *Appl. Math. Modell.* **15**, 136–143.

PARKHURST D. L., THORSTENSON D. C. and PLUMMER L. N. (1980) PHREEQE—A computerized program for geochemical calculations. U.S. Geol. Surv. Water-Resources Invest. 80-96.

SCHNOOR J. L. (1990) Kinetics of chemical weathering: A comparison of laboratory and field weathering rates. In *Aquatic Chemical Kinetics* (ed. W. STUMM), Chap 17, pp. 475–504. John Wiley & Sons, Chichester.

SILVERMAN M. P. (1967) Mechanism of bacterial pyrite oxidation. *J. Bacteriol.* **94**, 1046–1051.

SILVERMAN M. P. and LUNDGREN D. G. (1959) Studies of chemoautotrophic iron bacterium *Ferrobacillus ferrooxidans*, 2. Manometric studies. *J. Bacteriol.* **78**, 326–331.

SMITH E. E., SVANKS K. and SHUMATE K. S. (1968) Sulfide and sulfate reaction studies. 2nd Symp. Coal. Mine Drainage Res. Pittsburg, Pennysylvania.

STEGER H. F. and DESJARDINS L. E. (1978) Oxidation of sulfide minerals, 4. Pyrite, chalcopyrite and pyrrhotite. *Chem. Geol.* **23**, 225–237.

STRÖMBERG B., BANWART S., BENNETT J. W. and RITCHIE A. I. M. (1994) Mass balance assessment of initial weathering processes derived from oxygen consumption rates in waste sulfide ore. Paper presented at the International Land Reclamation and Mine Drainage Conference and the Third International Conference on the Abatement of Acidic Drainage, Pittsburgh, Pennysylvania, 24–29 April.

STUMM W. (1991) *Chemistry of the Solid–Water Interface*. John Wiley & Sons, Chichester.

STUMM W. and MORGAN J. J. (1981) *Aquatic chemistry*. John Wiley & Sons, Chichester.

STUMM W., MORGAN J. J. and SCHNOOR J. (1983) Acid-rain, a consequence of mass alteration of hydrogeochemical cycles. *Naturwissenschaften* **70**, 216–223.

SUNG W. and MORGAN J. J. (1980) Kinetics and product of ferrous iron oxygenation in aqueous systems. *Environ. Sci. Technol.* **14**, 561–568.

TAYLOR B. E., WHEELER M. C. and NORDSTROM D. K. (1984a) Isotope composition of sulphate in acid mine drainage as measure of bacterial oxidation. *Nature* **308**, 538–541.

TAYLOR B. E., WHEELER M. C. and NORDSTROM D. K. (1986b) Stable isotope geochemistry of acid mine drainage: Experimental oxidation of pyrite. *Geochim. cosmochim. Acta* **48**, 2669–2678.

TRUESDELL A. H. and JONES B. F. (1974) WATEQ a computer program for calculating chemical equilibria of natural waters. *J. Res. U.S. Geol. Surv.* **2**, 233–248.

VELBEL M. A. (1985) Geochemical mass balances and weathering rates in forested watersheds of the Southern Blue Ridge. *Am. J. Sci.* **285**, 904–930.

VIEILLARD P. (1988) Propriétés thermochimiques des composés du cuivre atlas de données thermodynamiques. *Sci. Geol. Bull.* **41**, 289–308.

VLEK P. L. G., BLOM T. J. M., BEEK J. and LINDSAY W. L. (1974) Determination of the solubility product of various iron hydroxides and jarosite by the chelation method. *Proc. Soil Sci. Am.* **38**, 429–432.

WEHRLI B. (1990) Redox reactions of metal ions at mineral surfaces. In *Aquatic Chemical Kinetics* (ed. W. STUMM), Chap 11, pp. 311–336. John Wiley & Sons, Chichester.

WHITE A. F. and PETERSON M. L. (1990) Role of reactive-surface-area characterization in geochemical kinetic models. In *Chemical Modeling of aqueous Systems II* (eds D. C. MELCHOIR and R. L. BASSETT), Chap 35, pp. 461–475. ACS Symposium Series 416.

WIELAND E., WEHRLI B. and STUMM W. (1988) The coordination chemistry of weathering: III. A generalization on the dissolution rates of minerals. *Geochim. cosmochim. Acta* **52**, 1969–1981.

WIERSMA C. L. and RIMSTIDT J. D. (1984) Rates of reaction of pyrite and marcasite with ferric iron at pH 2. *Geochim. cosmochim. Acta* **48**, 85–92.

WILLIAMSON M. A. (1992) Thermodynamic and kinetic studies of sulfur geochemistry. Ph.D. thesis, Virginia Polytechnic Inst. and State Univ., Chap. 4, pp. 92–133.

ZHANG Y., CHARLET L. and SCHINDLER P. W. (1992) Adsorption of protons, Fe(II) and Al(III) on lepidocrocite ($\gamma$ – FeOOH). *Colloid and Surfaces* **63**, 259–268.